Bioactive Materials 16 (2022) 47–56

Contents lists available at ScienceDirect

Bioactive Materials

journal homepage: www.keaipublishing.com/en/journals/bioactive-materials

Formulation of pH-responsive PEGylated nanoparticles with high drug loading capacity and programmable drug release for enhanced antibacterial activity

Dawei Li [a,b,1], Guoke Tang [c,1], Hui Yao [d,1], Yuqi Zhu [d], Changgui Shi [e], Qiang Fu [c,**], Fei Yang [b,f,*], Xing Wang [b,f,***]

[a] Senior Department of Orthopedics, The Fourth Medical Center of PLA General Hospital, Beijing, 100091, China
[b] Beijing National Laboratory for Molecular Sciences, State Key Laboratory of Polymer Physics & Chemistry, Institute of Chemistry, Chinese Academy of Sciences, Beijing, 100190, China
[c] Department of Orthopedics, Shanghai General Hospital, Shanghai Jiaotong University, Shanghai, 200080, China
[d] Department of Orthopedics, Eye Hospital China Academy of Chinese Medical Sciences, Beijing, 100040, China
[e] Department of Orthopedics, Second Affiliated Hospital of Naval Medical University, Shanghai, 20003, China
[f] University of Chinese Academy of Sciences, Beijing, 100049, China

ARTICLE INFO

Keywords:
pH-responsive prodrug
PEGylated
Programmable drug release
Schiff base
Antibacterial activity

ABSTRACT

In the current global crisis of antibiotic resistance, delivery systems are emerging to combat resistant bacteria in a more efficient manner. Despite the significant advances of antibiotic nanocarriers, many challenges like poor biocompatibility, premature drug release, suboptimal targeting to infection sites and short blood circulation time are still challenging. To achieve targeted drug delivery and enhance antibacterial activity, here we reported a kind of pH-responsive nanoparticles by simply self-assembly of an amphiphilic poly(ethylene glycol)-Schiff-vancomycin (PEG-Schiff-Van) prodrug and free Van in one drug delivery system. The acid-liable Schiff base furnished the PEG-Schiff-Van@Van with good storage stability in the neutral environment and susceptible disassembly in response to faintly acidic condition. Notably, on account of the combination of physical encapsulation and chemical conjugation of vancomycin, these nanocarriers with favorable biocompatibility and high drug loading capacity displayed a programmed drug release behavior, which was capable of rapidly reaching high drug concentration to effectively kill the bacteria at an early period and continuously exerting an bacteria-sensitive effect whenever needed over a long period. In addition, more Schiff-base moieties within the PEG-Schiff-Van@Van nanocarriers may also make great contributions on promoting the antimicrobial activity. Using this strategy, this system was designed to have programmable structural destabilization and sequential drug release due to changes in pH that were synonymous with bacterial infection sites, thereby presenting prominent antibacterial therapy both *in vitro* and *in vivo*. This work represents a synergistic strategy on offering important guidance to rational design of multifunctional antimicrobial vehicles, which would be a promising class of antimicrobial materials for potential clinical translation.

Peer review under responsibility of KeAi Communications Co., Ltd.
* Corresponding author. Beijing National Laboratory for Molecular Sciences, State Key Laboratory of Polymer Physics & Chemistry, Institute of Chemistry, Chinese Academy of Sciences, Beijing, 100190, China.,
** Corresponding author.
*** Corresponding author. Beijing National Laboratory for Molecular Sciences, State Key Laboratory of Polymer Physics & Chemistry, Institute of Chemistry, Chinese Academy of Sciences, Beijing, 100190, China.
E-mail addresses: Johson.f@163.com (Q. Fu), fyang@iccas.ac.cn (F. Yang), wangxing@iccas.ac.cn (X. Wang).
[1] These authors have contributed equally to this work.

https://doi.org/10.1016/j.bioactmat.2022.02.018
Received 1 January 2022; Received in revised form 15 February 2022; Accepted 15 February 2022
Available online 24 February 2022

1. Introduction

Bacterial infectious diseases pose a serious threat to global health and economics because of the accelerated emergence of antibiotic-resistant bacterial strains, which is considered one of the main contributors towards the gradually increasing morbidity and mortality rates [1,2]. More and more researches have pointed out that bacterial diseases can kill people than any others by 2050 [3,4]. Therefore, an urgent need is required for design of innovative antimicrobial biomaterials to curtail the present antibiotic-resistant pathogenic strains [5–7]. Generally, the traditional antibiotic dosage forms possess producible limitations like suboptimal drug concentration at infection sites, high exposure to healthy cells, low blood circulation time and the constraint of high doses required for efficient administration, which can cause the low-efficient drug delivery, inevitable adverse effects or toxicity and poor patient compliance, thus leading to the serious outcomes and antibiotic resistance [8–10]. Thereby, there is availability of advanced delivery strategy of smart drug delivery systems to improve drug loading capacity (DLC) and on-demand drug release are promising to decrease conventional dosage interval, improve drug bioavailability, reduce side effects and suppress the antimicrobial resistance.

Novel drug delivery system, because of its subcellular morphology, dimension, biocompatibility, biodegradability and surface area, has showcased their importance and efficiency in resolving the disadvantages of conventional antibiotics via improving the drug delivery and keeping high drug concentration at targeted bacterial infection sites [11–17]. Recently, responsive drug delivery has great potential in specific treatments by lowering the side effects and improving the efficacy. Since many bacteria (e.g. *Staphylococcus aureus* and *cariogenic* bacteria) can produce acids at the infection site by the combined actions of immune response and bacterial metabolism, pH trigger is recognized as an attractive strategy on the targeted antibiotic delivery in the antimicrobial arsenal, and thereby pH-responsive antibiotics release can effectively suppress the drug-resistance and reduce the cytotoxicity [18–24]. Using this strategy, design and development of therapeutic systems that respond to pH trigger are significantly important for enhancing antibacterial efficacy. Among the various drug carriers, prodrug-based nanoparticles have emerged as an outstanding candidate because of their clear structure and simple synthetic procedure in clinical translation. Wherein, Schiff base-linked degradable prodrugs are of particular interest due to their reversible dynamic bonds between the aldehyde and amino groups, which can quickly hydrolyze under a weakly acidic condition and native antimicrobial secretion [25–28]. In particular, rapid growth of bacteria can produce lactic acid in its metabolic process, resulting in local weak acidification, and therefore Schiff base-linked polymeric carrier is suitable for constructing bacteria-sensitive antibiotics release system.

Vancomycin is a first-generation glycopeptide antibiotic with broad-spectrum abilities to keep sustained microbiologic inhibitory activity via inhibiting the synthesis of bacterial cell wall. It has no cross-resistance to other antibiotics and rarely generates resistant strains that is recognized as an effective antibiotic for most Gram-positive bacteria in the critical situation medicine [29–31]. DLC and drug release kinetics are of great importance to drug delivery systems. To tackle this challenge, innovative strategies have been explored for developing advanced nanocarriers with high DLC and tailored drug release kinetics related to the drug concentration and the time of drug action [32–34]. To maximize the bacteria growth inhibition, it is necessary to achieve high drug concentration at the infection sites and keep programmed drug release for a long period, which meant the rapid drug release to enhance the local drug concentration to urgently kill the bacteria in the initial stage, and responsive release of antibacterial drug to treat and/or prevent further bacterial infection in the middle or later periods, resulting in efficient antibiotic delivery and outstanding therapeutic effects. Therefore, development of programmable drug delivery with particular emphasis on high drug concentration loading and sequential release is significantly urgent for enhanced antibacterial therapy.

Herein, we designed and prepared a pH-responsive prodrug from an amphiphilic polymer drug conjugate, poly(ethylene glycol)-Schiff-vancomycin (PEG-Schiff-Van) via the simple chemical synthesis procedures. This PEGylated prodrug could serve as drug carrier to further encapsulate the free vancomycin in one drug delivery system (PEG-Schiff-Van@Van), which exhibited good biocompatibility, well-defined architectures, high drug loading content, stability and storage. The bridged Schiff bases could keep the structural integrity at normal physiological condition but quickly disassemble in response to faintly acidic environment. More importantly, the combination of physical encapsulation and chemical conjugation endowed the nanoparticles with an efficient drug load concentration and a programed drug release behavior, thus achieving the on-demand antibiotics release for targeted antimicrobial activity (Fig. 1). Thus, we believe that these prodrug nanomedicines will hold promise to an alternative translational antibiotic formulation for effective antimicrobial therapy.

2. Materials and methods

2.1. Materials

Poly(ethylene glycol) methyl ether (PEG-OH, M_n = 750 g/mol, Alfa Aesor), 4-carboxybenzaldehyde (98%, J&K), 4-(dimethyl-amino)-pyridine (DMAP, 99%, Aldrich), 1-(3-dimethylaminopropyl)-3-ethyl-carbodiimide hydrochloride (EDCI, 99%, Energy Chemical), Vancomycin (Van, 95%, TCI), N,N-diisopropylethylamine (DIEA, 98%, Energy Chemical), hydrochloric acid, sodium sulfate, n-hexane and ether were purchased from Beijing Chemical Works. Dichloromethane (DCM) and dimethylformamide (DMF) were purified by stirring over calcium hydride for 24 h followed by distillation. All other reagents were purchased from Sigma-Aldrich and used as received without further purification. *Staphylococcus aureus* (*S. aureus*, ATCC 29213) was purchased from institute of microbiology, Chinese Academy of Sciences, Beijing, PR China. All cells were supplied by China Infrastructure of Cell Line Resource.

2.2. General characterizations

Nuclear magnetic resonance (NMR) spectra were recorded on a Bruker 400 MHz spectrometer with tetramethylsilane (TMS) as the internal reference. Transmission electron microscopy (TEM) images were obtained on a JEM-2200FS microscope (JEOL, Japan). A 5 μL droplet of self-assembled solution was dropped onto a copper grid (300 mesh) coated with a carbon film, followed by drying at room temperature. Dynamic light scattering (DLS) spectra were obtained on a commercial laser light scattering spectrometer (ALV/DLS/SLS-5022F) equipped with a multi-τ digital time correlator (ALV5000) and a cylindrical 22 mW UNIPHASE He–Ne laser (λ_0 = 632.8 nm) was used. All data were averaged over three time. The laser light scattering cell was held in a thermostat index matching vat filled with purified and dust-free toluene, with the temperature controlled to within 0.1 °C. Fluorescence measurement was carried on a Hitachi F4600 photo-luminescent spectrometer with a xenon lamp as a light source. Confocal laser scanning microscopy was obtained on a Zeiss LSM 510 microscope.

2.3. Synthesis of the PEG-CHO polymer

PEG-OH (1.5 g, 2 mmol), 4-carboxybenzaldehyde (0.36 g, 2.4 mmol), EDCI (0.48 g, 2.4 mmol) and DMAP (50 mg, 0.4 mmol) were added into a 20 mL of freshly dried DCM equipped with a magnetic stirring bar. After continuous stirring for 24 h at room temperature, the organic phase was collected and washed with 2 M HCl aqueous solution, saturated NaCl aqueous solution and DI water for several times and dried over anhydrous Na_2SO_4 [27]. The final product was precipitated into ether/hexane for three times to afford the white powder with 86.6%

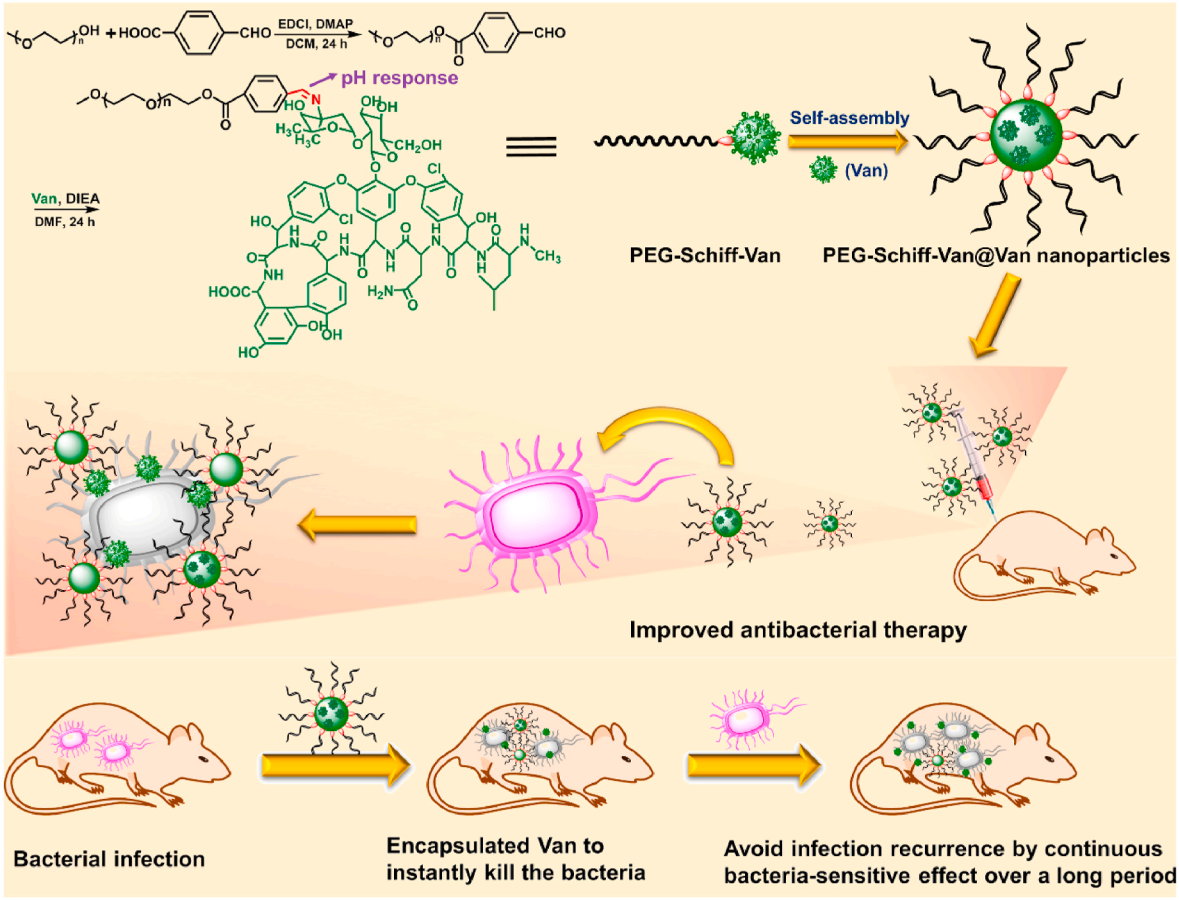

Fig. 1. Schematic illustration of preparation of PEG-Schiff-Van@Van nanoparticles for programmable antibacterial therapy.

yields.

2.4. Synthesis of the PEG-Schiff-Van polymer

PEG-CHO (0.36 g, 0.4 mmol), Van (0.3 g, 0.2 mmol) and DIEA (70 μL, 0.4 mmol) were dissolved in 10 mL of DMF solution under a nitrogen atmosphere. After refluxing for 12 h, the solvent was removed and the crude products were resolved in DCM, which was then washed with saturated NaCl aqueous solution and DI water for several times and dried over anhydrous Na_2SO_4. The final product was precipitated into ether for several times to afford the white powder with 66.4% yields.

2.5. Self-assembly of the PEG-Schiff-Van and PEG-Schiff-Van@Van nanoparticles

A typical self-assembly solution was prepared as following: PEG-Schiff-Van (5 mg) was first dissolved in DMF (1 mL), then the deionized water (4 mL) was added dropwise into the solution at the rate of 0.05 mL/min via a syringe pump. The colloidal dispersion was further stirred for another 2 h at room temperature during the self-assembling process. Afterwards, the organic solvent was removed by dialysis (MW cutoff, 2 kDa) against deionized water for 3 days to obtained the PEG-Schiff-Van nanoparticles.

Similarly, 5 mg of PEG-Schiff-Van and a predetermined amount of free vancomycin was dissolved in 1 mL of DMF, and then 4 mL of deionized water was added dropwise into the solution at the rate of 0.05 mL/min via a syringe pump. The colloidal dispersion was further stirred for another 2 h at room temperature during the self-assembling process. Afterwards, the organic solvent and free Van was removed by dialysis (MW cutoff, 2 kDa) against deionized water for 3 days to obtain the PEG-Schiff-Van@Van nanoparticles.

To determine the final concentration of Van and the encapsulation efficiency, 0.1 mL of the solution was diluted to 5 mL by adding mixture of trifluoracetic acid: acetonitrile (v/v = 15:85). After being vibrated at 37 °C for 24 h to make the vancomycin release completely, the concentration of Van was determined by high performance liquid chromatography (HPLC). The encapsulation efficiency of Van in the nanoparticle solutions could be calculated according to the measured concentration.

2.6. Dissipative particle dynamics (DPD) simulation

DPD was performed to understand the assembly of the molecule in water [37]. First of all, we constructed a specific coarse-grained (CG) model of the molecule wherein one bead P (representing PEG) attached to another bead V (representing vancomycin). The atomistic model was coarse-grained according to the molecular volumes which were computed in all-atom simulation. The size of V bead is 1.31 times of P bead. The interaction parameter a_{ij} between different beads was presented in the following table.

a_{ij}	P	V	W
P	25	100	25
V		25	100
W			25

Within the CG model, neighboring CG beads are bonded to each other by a harmonic spring potential, $U_b = 0.5k_b(r - r_0)^2$, where k_b is the spring constant and r_0 is the equilibrium bond length. In this study, $k_b = 25$ and $r_0 = 2.0$. The concentration of the molecule in the solution

φ is 0.009, which is calculated by the following formula.

$$\varphi = \frac{N_V V_V + N_P V_P}{N_V V_V + N_P V_P + N_W V_W}$$

where N_V, N_P and N_W are the number of the vancomycin, PEG and water beads while V_V, V_P and V_W are the volume of one bead of vancomycin, PEG and water, respectively.

The simulations were performed in NVT ensemble with periodical boundary conditions and at a fixed system number density of 3.0. All the CG beads have the same mass as m = 1. The interaction cutoff radius is set to 1 as the unit of length. The temperature is 1.0. The size of simulation box is 30 × 30 × 30. In the DPD simulations the modified velocity-verlet algorithm was used to integrate the equations of motion with a time step of 0.03. The simulation systems were pre-equilibrated with 1 × 10^5 steps by setting a_{ij} = 25 and T = 1.0 for all DPD beads. Then we performed another simulation with 4 × 10^6 steps to observe the morphology evolution of aggregates. In the equilibrium state, we observed spherical aggregates.

2.7. pH-responsive profile of PEG-Schiff-Van and PEG-Schiff-Van@Van nanoparticles

For determining the pH response of PEG-Schiff-Van and PEG-Schiff-Van@Van nanoparticles, a certain amount of phosphate buffered saline (PBS) with different pH values (6.0 and 7.4) was added into 10 mL of PEG-Schiff-Van or PEG-Schiff-Van@Van nanoparticles (1 mg/mL) under mildly stirring at 37 °C. After 4 h, morphological and dimensional changes of nanoparticles were characterized by TEM and DLS.

2.8. In vitro release from the PEG-Schiff-Van and PEG-Schiff-Van@Van nanoparticles

pH-triggered Van release was conducted as below: dispersed PEG-Schiff-Van or PEG-Schiff-Van@Van nanoparticles were added into a dialysis membrane tube (MW cutoff, 2 kDa), which was then incubated in 30 mL of PBS (pH 6.0 and 7.4) solutions at 37 °C in a shaking water bath. Release profiles were determined by HPLC at 230 nm. All release experiments were performed in triplicate.

2.9. In vitro cytotoxicity

The cytotoxicity of PEG-Schiff-Van nanoparticles was conducted by CCK-8 assay. Mouse embryos osteoblast precursor cells (MC3T3-E1) were seeded onto a 96-well plate at a density of 1 × 10^4 cells per well in 200 μL of DMEM containing 10% FBS for incubation of 24 h (37 °C, 5% CO_2). The medium was replaced by 90 μL of fresh DMEM medium containing 10% FBS, followed by adding various concentration of suspensions (pH 7.4) for another incubation of 24 h. After the removal of culture media from cell culture plates, 100 μL of fresh culture media and 10 μL of CCK-8 kit solutions were immediately added and incubated for 4 h. The optical density of each well at 450 nm was read by a microplate reader. Cells cultured in DMEM medium containing 10% FBS (without exposure to sample) were used as controls.

2.10. Confocal laser scanning microscopy (CLSM) observation

MC3T3-E1 cells were seeded into 24-well culture plates to incubate for 24 h at 37 °C in humidified air containing 5% CO_2. Using the DMEM (Dulbecco's modified Eagle's medium) with 10% FBS, 50 IU mL^{-1} penicillin and 50 IU mL^{-1} streptomycin of the culture media were replaced by PEG-Schiff-Van solutions (200 μg/mL). After cultivating for prescribed time intervals, the MC3T3-E1 cells were washed by cold buffer for three times and immersed with 4% paraformaldehyde solution for 0.5 h to fix the cell configuration. Afterwards, 4,6-diamidino-2-phenylindole (DAPI) was employed for cellular staining and the MC3T3-E1 cells were washed by buffer for three times and directly transferred into culture dish for further CLSM observation.

2.11. Inhibition zone measurement

Inhibition zone was measured by placing the bacterial solution on the surface of an agar plate. Then each tested antibacterial agent samples were respectively filled into the circle, and bare vancomycin drug (pH 7.4, 6 h) and four PEG-Schiff-Van@Van nanoparticles (pH 7.4, 6 h, pH 7.4, 24 h, pH 6.0, 6 h and pH 6.0, 24 h) were placed on the inoculated agar plates and incubated overnight at 37 °C. Digital images of plates were captured to measure the inhibition zone diameter. Each experiment was preceded in triplicate [35].

2.12. Antibacterial experiments

Bare vancomycin drug, PEG-Schiff-Van and PEG-Schiff-Van@Van nanoparticles were incubated with the *S. aureus* for different incubation concentration at various times (6 h and 24 h). After being washed and diluted with PBS buffer, the bacteria dilutions were spread onto a solid LB agar plate. The bacterial colonies were formed after 18 h incubation at 37 °C. Each group was performed in triplicate. The bacterial viability was calculated as follows:

$$\textbf{Bacterial viability} = \frac{\textbf{number of CFU (treated)}}{\textbf{number of CFU (control)}} \times 100\%$$

2.13. Live/dead staining

The antibacterial activities of bare vancomycin and PEG-Schiff-Van@Van nanoparticles were determined by incubation with bacterial cells suspensions at room temperature. A ratio of strain dyes was added to the samples and kept for 15 min. The used bacteria stains were SYTO 9 (green fluorescence) for Gram-positive bacteria and propidium iodide (PI, red fluorescence). Bacteria with intact cell membranes were stained green, and bacteria with damaged membranes were stained red for further CLSM observation.

2.14. In vivo antimicrobial assay

All experiments were performed in accordance with the Guidelines of the care and use of laboratory animals of 8th Medical Center of Chinese PLA General Hospital, and Experiments were approved by the animal ethics committee of the 8th Medical Center of Chinese PLA General Hospital. The wounds (1 cm × 1 cm) were made using puncher on the back of each rat, followed by adding the *S. aureus* (200 μL) (1 × 10^8 CFU mL^{-1}). After 24 h, the infection sites were treated with separately nanoparticle solutions (100 μg/mL, 100 μL) and the same volume of PBS. The rats were euthanized on 7 and 14 days, and the skin was fixed with 10% buffered formalin. The sections were stained by Hematoxylin−Eosin (H&E), Masson's trichrome reagents, CD31 and CD68 antibody [36].

3. Results and discussion

3.1. Synthesis and characterization of PEG-Schiff-Van prodrugs

The Schiff-linked PEGylate Van prodrug was prepared following the synthetic route as seen in Fig. 1. Based on the simple esterification reaction of 4-carboxybenzaldehyde and sequentially high-effective Schiff base reaction of Van, the PEG-Schiff-Van was feasibly obtained with the verification by ^{1}H NMR spectra. Fig. 2A presented the clear assignments of PEG-CHO polymer. The signals at δ 8.0–8.3 ppm ascribed to the benzene components and the resonance peak of δ 10.2 ppm was attributed to the proton of aldehyde group. There was no clear peak attribution in Fig. 2B because of the intricate peaks for free vancomycin

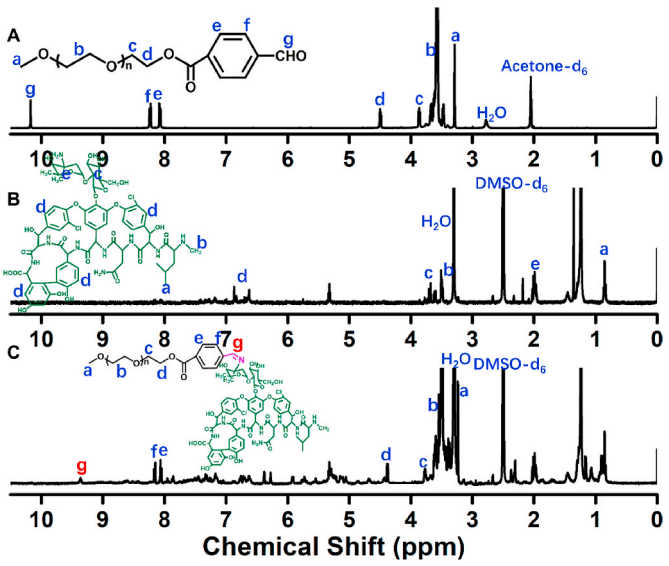

Fig. 2. ^{1}H NMR spectra of (A) PEG-CHO, (B) Van and (C) PEG-Schiff-Van polymers.

drug. Fig. 2C proved the successful conjugation of PEG with Van via the Schiff base reaction, presenting the integrated assignments of PEG (δ 3.3 ppm and 3.5–4.1 ppm) and Van moieties (similar to Fig. 2B). The newly generated peak at δ 8.4 ppm for Schiff base bond and the completely disappeared signal of aldehyde group at δ 10.2 ppm fully testified the successful preparation of PEG-Schiff-Van polymer. Especially, the integration ratio of representative characteristic peaks further certified its exact and identical structure. The Van content in the PEG-Schiff-Van prodrug was calculated to be 62.7 wt%, higher than most of other reported Van prodrugs, which was sufficient for therapeutic usage.

3.2. Preparation, stability and pH-responsive degradation of the nanoparticles

PEG-Schiff-Van prodrug could self-assemble into micellar nanoparticles in aqueous solutions because of its amphiphilic structure and high uniformity, which was well demonstrated by TEM image in Fig. 3A–a. These nanoparticles had a particle size of ca. 85 nm and a polydispersity index (PDI) of 0.22 by DLS result in Fig. 3B–a. Dissipative particle dynamics (DPD) simulation is currently recognized as the viable simulation approach that can be employed to intuitively study the macromolecular morphological expressions [37], which provided a visualized formation pathway of the self-assembled nanoparticles from the amphiphilic PEG-Schiff-Van prodrug (Fig. 3C). To maximally increase Van content in the nanoparticles, free vancomycin was further *in situ* encapsulated into the micelles to form the PEG-Schiff-Van@Van nanoparticles, which exhibited the larger average hydrodynamic size than PEG-Schiff-Van prodrug by DLS (ca. 106 nm) in Fig. 3A–b and 3B-b. These polymeric nanoparticles possessed outstanding storage stability that was important for the drug formulations although there was some degree of micellar swelling in aqueous solutions (Fig. 3D), however, they were susceptible to disassemble under faintly acidic condition because of the acid-labile Schiff base linker within the nanoparticles. After incubation in pH 6.0 PBS solutions for 4 h, Fig. 3A–c showed the morphological degradation in the presence of pH 6.0 solutions, and the small molecules and aggregates were observed in Fig. 3B–c, confirming pH-induced cleavage of Schiff base bonds and dissociation of the aggregates. Therefore, these kinds of pH-sensitive nanoparticles could keep stable at normal physiological conditions and degradable in response to acidic conditions, which may be used as the intelligent drug carriers in biomedical fields.

3.3. In vitro biocompatibility and drug release of the nanoparticles

CCK-8 assay was used to evaluate the *in vitro* cytotoxicity of PEG-Schiff-Van. After incubation for 24 h using MC3T3-E1 cells, cell viability was more than 90% until the tested concentration reached 200 μg/mL, which displayed the healthy cell morphology and emitted green fluorescence (Fig. 3E and F), demonstrating good *in vitro* biocompatibility and usability of this prodrug. Since the acid-labile linker between the hydrophobic Van and the hydrophilic PEG was susceptible to disassemble under faintly acidic condition, we assessed the drug release profiles of PEG-Schiff-Van and PEG-Schiff-Van@Van nanoparticles at the physiological (PBS, pH 7.4) and acidic conditions (PBS, pH 6.0) to simulate the severe infection environment. As depicted in Fig. 3G, a negligible vancomycin was released from the PEG-Schiff-Van nanoparticle at pH 7.4 solutions while a much faster release of Van with a high release content of 82.2% at pH 6.0 solutions, which was attributed to the cleavage of Schiff base to accelerate the vancomycin release, indicating that these prodrugs would maintain stable and eliminate the premature burst release in normal environment while effectively promote the vancomycin release upon exposure into acidic environment.

Recent developments in smart drug carriers for antimicrobial therapy have enabled programmable delivery of therapeutics by means of stimuli-responsive behavior. It is greatly desired to construct an ideal criterion that the designed drug delivery system should quickly achieve high drug concentration to kill the bacteria at an early period and exert an environmental responsive effect whenever needed to avoid recurrence of infection for a long period of time. So, we further prepared the PEG-Schiff-Van@Van nanoparticles by incorporation of encapsulated Van and conjugated Van in one drug delivery system, which was expected to achieve the rapid release of encapsulated vancomycin to enhance local drug concentration at first stage within a short time, and then conduct the pH-responsive release of chemically conjugated vancomycin to continue the effective treatment or prevent the recurrence of infection, thereby resulting in intelligent therapeutic effect. The drug loading capacity was 68.4% from the results determined by HPLC measurements. As expected, PEG-Schiff-Van@Van nanoparticles indeed displayed a sequential drug release behavior in Fig. 3H. The 26.2% of vancomycin release from the nanoparticles was accordance with its physical drug loading content, indicating the initial drug concentration gradient diffusion behavior of encapsulated Van at the neutral environment and verifying the following sustained drug release with nanoformulation due to the possible polymer erosion and degradation. While treatment in harsh pH 6.0, accumulative vancomycin release was dramatically accelerated to reach 92.6%, which suggested nearly all the encapsulated Van and conjugated Van were released. The fast Van release was attributed to the fact that deprotonated vancomycin in the interior could easily escape from the broken carriers at acidic pH. Besides, the release of encapsulated Van just continued for 24 h, whereas the release of conjugated vancomycin could sustain for more than 60 h, which suggested their enhanced antibacterial activity in clinical application scenarios that required the high concentration of antibiotics on the effective inhibition of bacteria growth from infected wounds or locally continuous drug release for a long-term prevention of wound reinfection in the neutral environment. Overall, in contrast to the conventional vancomycin formulations with poor stability, premature drug burst release and insufficient therapeutic dose, these pH-responsive nanoparticles exhibited good stability, high drug loading contents, specific target transport and spatiotemporally controlled release to significantly reduce the drug-resistance and promote the antibacterial therapeutic effect. Using this strategy, these therapeutic systems can be designed with the relevant chemical and physical properties that respond to pH trigger for improving antibacterial efficacy, which are capable of programmable destabilization and on-demand release of the drug once the pH changes in bacterial infection sites.

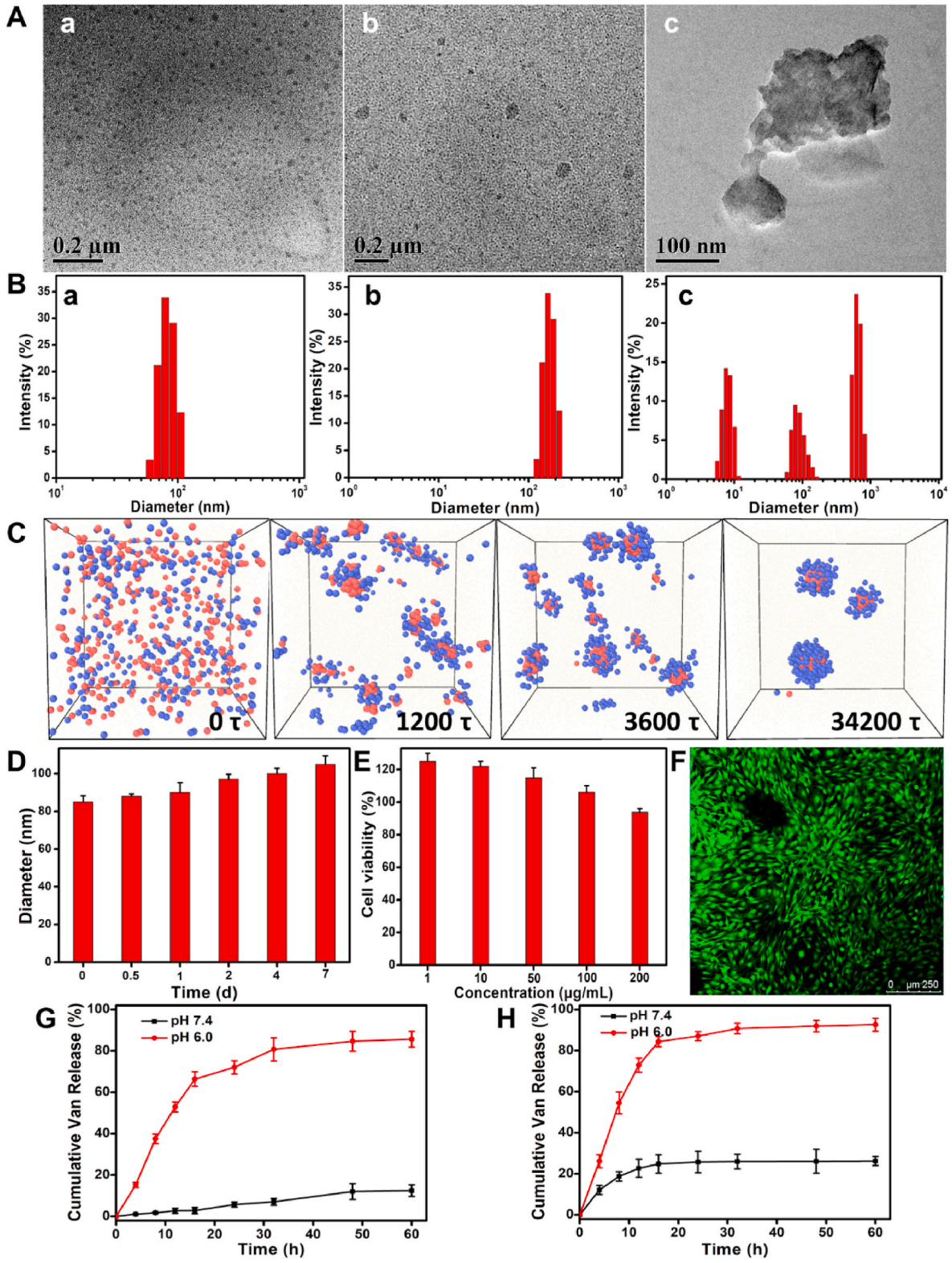

Fig. 3. (A) TEM images and (B) Size profiles of the PEG-Schiff-Van (a) and PEG-Schiff-Van@Van nanoparticles before (b) and after (c) treatment of pH 6.0 PBS solutions for 4 h. (C) The snapshots showing the formation pathway of nanoparticles. The water beads are omitted for clarity. (D) Size variations of the PEG-Schiff-Van nanoparticles after treatment in PBS (pH = 7.4) solutions for various time. (E) Cytotoxicity of MC3T3-E1 cells following 24 h incubation with PEG-Schiff-Van nanoparticles. (F) CLSM image of MC3T3-E1 cells cultured in the presence of 200 μg/mL of PEG-Schiff-Van nanoparticles. pH-triggered drug release from the (G) PEG-Schiff-Van and (H) PEG-Schiff-Van@Van nanoparticles after treatment in PBS (pH = 7.4 and 6.0) solutions.

3.4. Inhibition zone measurement and in vitro antimicrobial assay

Inhibition zone measurement was carried out to verify the antibacterial property against *staphylococcus aureus* (*S. aureus*). As shown in Fig. 4A, PEG-Schiff-Van@Van exhibited obvious inhibition haloes with effective antibacterial activity. In accordance with the drug release behavior in Fig. 3H, the sustainable vancomycin release in the first 6 h exhibited obvious antibacterial effect with a small inhibition zone at pH 7.4. After incubation for 24 h, the inhibition zone diameter was enlarged from 7 to 11 mm originating from the accumulative drug concentration by the diffusion behavior or generative weak acidic conditions from bacterial metabolism (Fig. 4A–a,4A-b and Fig. 4C). At pH 6.0, the obvious antibacterial inhibition as well as the large inhibition zone were showcased at 6 h, and further expanded into 12.5 mm after 24 h of incubation (Fig. 4A–c, 4A-d and Fig. 4C), which was attributed to the cleavage of Schiff base bonds and disassembly of the nanoparticles to accelerate the vancomycin release. In addition, it was reported that the Schiff base could play a role in facilitating the antibacterial therapy [26]. As a control, the bare vancomycin with nearly equivalent concentration (8 μg/mL) to that of physical encapsulation of PEG-Schiff-Van@Van nanoparticles displayed the effective antibacterial inhibition in Fig. 4A–e. The larger inhibition zone diameter (8.8 mm) than that of PEG-Schiff-Van@Van nanoparticles (7 mm, Fig. 4A–a) indicated the gradual drug release process, which also verified the promoting antibacterial capacity of Schiff base bonds and meanwhile suggested a few breaks of Schiff base bonds within the nanoparticles after incubation for 24 h. Therefore, more Schiff-base moieties within these nanocarriers could make great contributions on promoting the antimicrobial activity.

The antimicrobial efficiency of PEG-Schiff-Van@Van nanoparticles was further intuitively proved by confocal laser scanning microscopy. Live/dead bacterial viability assay was employed to observe the antibacterial activity. The green SYTO 9 dye could enter the both intact and membrane-compromised cells, whereas the red propidium iodide (PI) dye could only enter the membrane-compromised cells [38], which can be observed in the negative control group using PBS 7.4 solutions and positive control group with bare vancomycin drug in presence of SYTO 9 and PI dyes. When the *S. aureus* bacterial suspension was mixed with 100 μg/mL PEG-Schiff-Van@Van solutions at 37 °C, the resulting suspension of viable and dead bacteria was applied to a glass slide and treated with the combination dyes. Similar to the inhibition zone measurement, the number of viable cells (stained green) was gradually

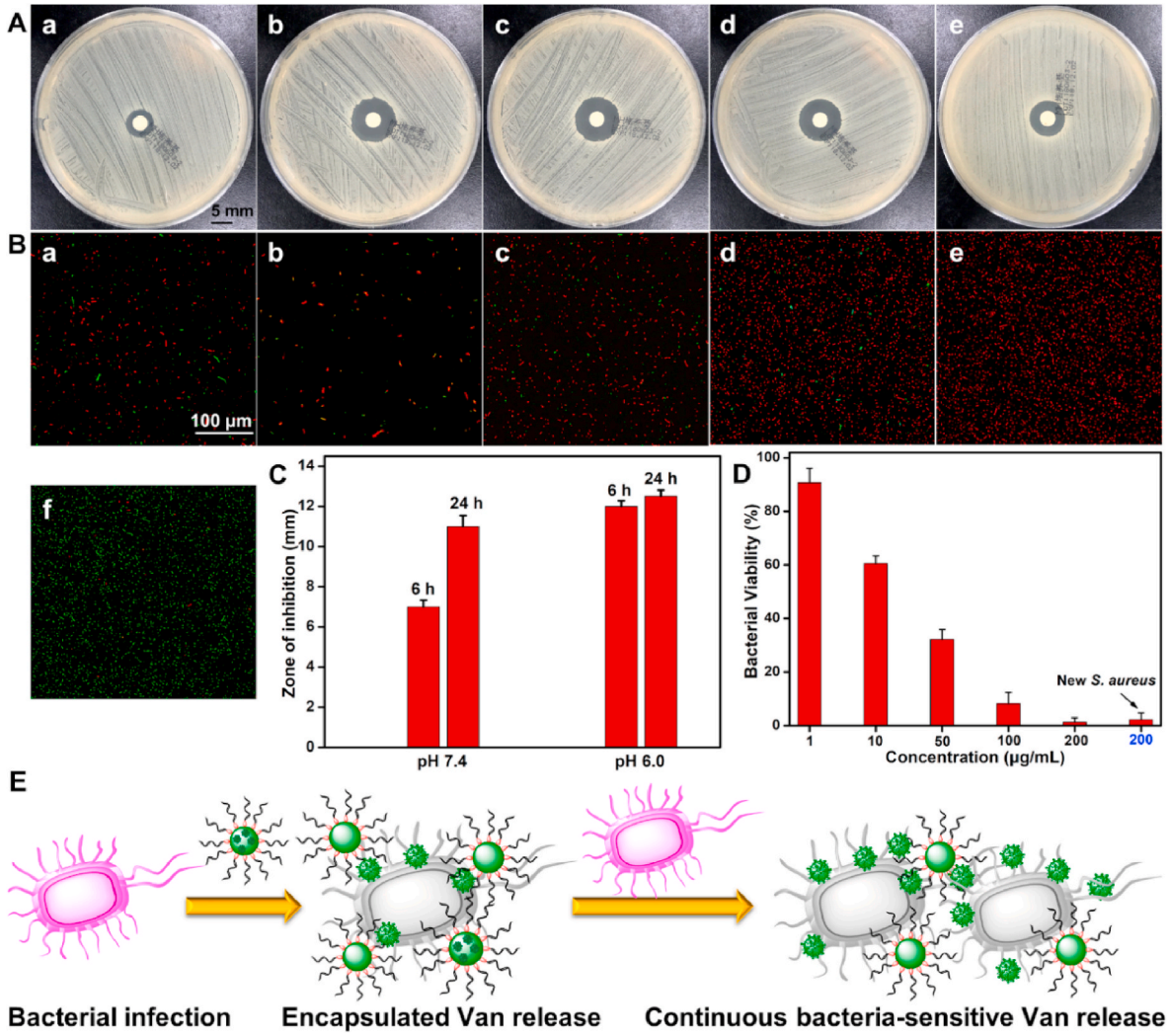

Fig. 4. (A, C) Representative inhibition zone and (B) Live/dead fluorescence staining images of *S. aureus* treated with PEG-Schiff-Van@Van nanoparticles (100 μg/mL) at (a) pH 7.4, 6 h, (b) pH 7.4, 24 h, (c) pH 6.0, 6 h and (d) pH 6.0, 24 h; (e) bare vancomycin drug (8 μg/mL) and (f) PBS at pH 7.4, 6 h. Red and green fluorescence represent dead and viable bacteria. (D) Quantitative analysis of the antibacterial activity of PEG-Schiff-Van@Van nanoparticles toward *S. aureus*. (E) Scheme of the PEG-Schiff-Van@Van nanoparticles with high drug concentration at the infection sites to instantly kill the bacterial and continuous bacterial-responsive drug release for programmable antimicrobial therapy.

reduced over time at pH 7.4 while red fluorescence intensities tended to be stronger and majority of the cells were stained red at pH 6.0 (Fig. 4B), indicative of the pH-responsive enhanced antibacterial activity. On account of the high drug loading and more Schiff-base moieties, PEG-Schiff-Van@Van nanoparticles with a low concentration (200 μg/mL) could effectively kill 99% of *S. aureus* in Fig. 4D, further indicating the efficient biocidal activity for the living *S. aureus*. It was mentioned that when the new *S. aureus*. fluid was repoured into these nanoparticles after 5 d that simulated the recurrence of infection, the antimicrobial activity was also remarkable, which was attributed to the environmental responsive effect and programmable delivery of therapeutics for antimicrobial therapy over a long period (Fig. 4E).

3.5. In vivo antibacterial activity

To observe the antimicrobial activity and wound healing, we employed a rat skin wound infection model using *S. aureus* to evaluate the antibacterial effect of nanoparticles *in vivo*. After 24 h of infection, the wounds of rat's back were separately treated with PBS, Van, PEG-Schiff-Van and PEG-Schiff-Van@Van. On the 7th day, the wound area in the treatment group (PEG-Schiff-Van@Van) was smallest than that in the other groups, and had nearly disappeared on the 14th day while the others were not completely healed (Fig. 5A). Hematoxylin and eosin (H&E) staining showed the bare scar after treatment on the 7 and 14th day. The rats in the PEG-Schiff-Van@Van group formed a relatively intact epidermis while other groups displayed the parakeratosis, epidermal hyperplasia and inflammatory infiltration with varying degrees (Fig. 5B). In addition, the formation of collagen fiber was further proved by Masson's staining in Fig. 5C. The continuous and ordered collagen fibers in the wound area were shown in the PEG-Schiff-Van@Van group, whereas disorganized and sparse collagen fibers appeared in the other groups. These results indicated the low drug utilization ratio for free vancomycin group. As for the PEG-Schiff-Van group, the low drug concentration in the early stage may impair its therapeutic effect, which reflected the programmable importance of drug gradient release. To detect the inflammation in the wound, CD68 expression was selected as a marker of monocyte infiltration (Fig. 5D), suggestive of that the CD68 expression (red dots) of PEG-Schiff-Van and PEG-Schiff-Van@Van was both apparently decreased from 7 to 14 days in the wound-infecting skin. Also, CD31 is an endothelial cell marker that reflected the formation of new capillary. Thus, the expression of CD31 (green) in wounds was analyzed to estimate the revascularization of the wound area. CD31-positive cells were largely found in the PEG-Schiff-Van@Van groups, and CD31-positive cell rates were found to be higher with time (Fig. 5E). These data demonstrated that PEG-Schiff-Van@Van nanoparticles could effectively suppress inflammatory response locating at the *in vivo* wound site and accelerate wound regeneration, which further proved the importance of high dose antibiotics loading and programed drug release capacities on the bacteria elimination once pH value was changed at the bacterial infection sites.

4. Conclusion

In summary, we developed a self-assembling PEGylated vancomycin prodrug of PEG-Schiff-Van via the conjugating hydrophobic Van into a short PEG chain. Incorporation of Schiff base into the polymeric architectures furnished the polymeric nanoparticles with pH responsiveness that maintained the structural integrity at neutral conditions and quickly disassembled in acidic conditions. After further encapsulation of free vancomycin drug through the self-assembly in the solutions, the PEG-Schiff-Van@Van nanoparticles was constructed with good biocompatibility, high drug loading capacity and on-demand drug release behaviors. Remarkably, benefitting from the combination of physical encapsulation and chemical conjugation, these PEG-Schiff-Van@Van nanoparticles exhibited a programed drug release behavior that could reach high drug concentration to kill the bacteria at an early period and exert an environmental responsive effect whenever needed over a long period. This multifunctional drug delivery system could effectively suppress the bacteria growth with excellent antibacterial activity against *S. aureus* and also facilitate the wound healing. *In vivo*

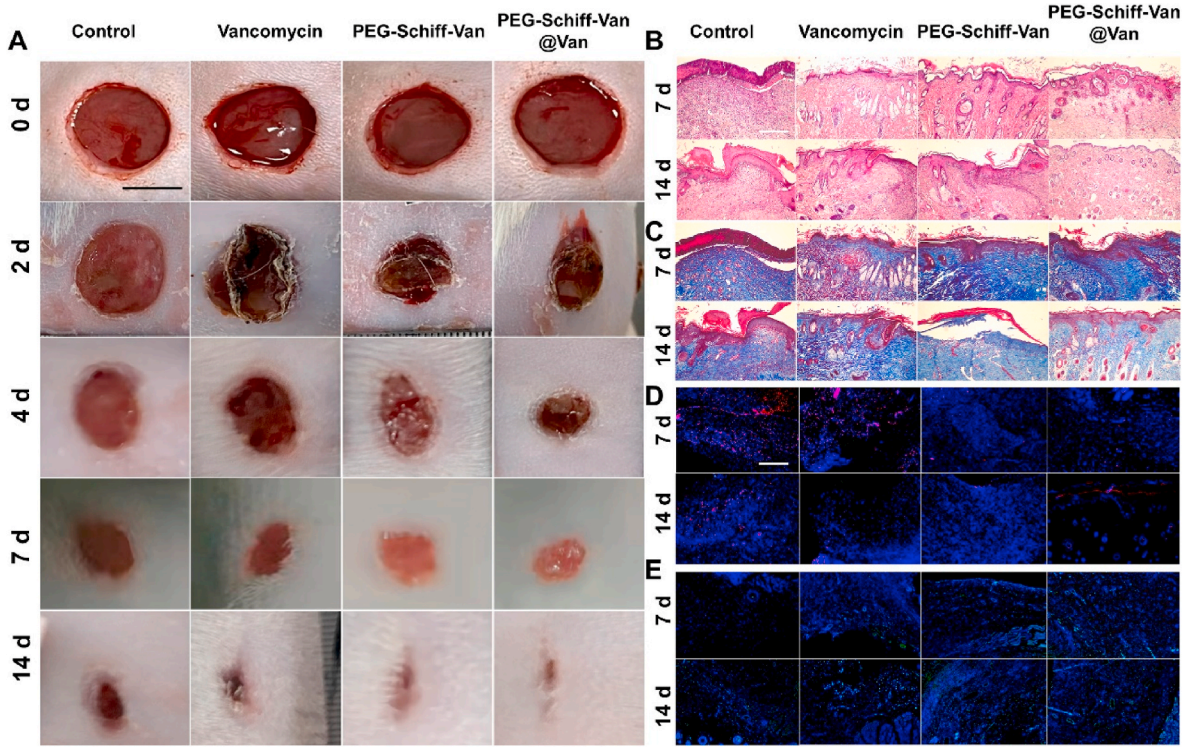

Fig. 5. Scheme of bacterial kill using *S. aureus*-infected SD rat models. (A) Photographs of wound closure on 0, 2, 4, 7, and 14 days *in vivo*. Scale bar = 0.5 cm. (B) H&E staining, (C) Masson's staining, (D) CD68 staining (red) and (E) CD31 staining (green) of tissue sections on 7 and 14 days. Scale bar = 200 nm.

results showed a favorable healing process with a reduced inflammation response in the surrounding tissues and reconstructed injured skin tissues. Taken together, this current work offers an effective antibacterial therapeutic modality for the treatment of infectious wounds with on-demand antibiotics release, which provides a promising option for construction of multifunctional drug delivery systems and development of translational vancomycin formulations to enhance the antibacterial therapy.

Declaration of competing interest

The authors declare no competing financial interest.

CRediT authorship contribution statement

Dawei Li: Conceptualization, Investigation, Methodology, Project administration, Writing – original draft. **Guoke Tang:** Data curation, Formal analysis, Investigation, Writing – review & editing. **Hui Yao:** Methodology, Investigation, Resources, Writing – review & editing. **Yuqi Zhu:** Data curation, Methodology. **Changgui Shi:** Data curation, Investigation. **Qiang Fu:** Resources, Methodology, Writing – review & editing. **Fei Yang:** Writing – review & editing. **Xing Wang:** Project administration, Funding acquisition, Supervision, Writing – review & editing.

Declaration of competing interest

The authors declare no conflict of interest.

Acknowledgements

This work was supported by Youth Innovation Promotion Association CAS (2019031), National Natural Science Foundation of China (51973226, 81972081 and 21604093), China Postdoctoral Science Foundation (2020M683733), Military Medical Science and Technology Youth Cultivation Project (20QNPY109), Military Medical Youth Growth Program of PLA General Hospital (QNC19028), and Shanghai Changning Committee of Science and Technology of China (CNKW2020Y01). The authors also thank Prof. Hongxia Guo, Dr. Chong Yu and Peiyuan Gao for the DPD simulation analysis.

References

[1] G. Rahimzadeh, P. Gill, M.S. Rezai, Cysteine/histidine-dependent amidohydrolase/peptidase (CHAP)-Displayed nano phages: antimicrobial function against methicillin-resistant Staphylococcus aureus (MRSA), Avicenna J. Med. Biotechnol. 12 (2020) 85–90.

[2] X. Zhen, L. Chudal, N.K. Pandey, J. Phan, X. Ran, E. Amador, X. Huang, O. Johnson, Y. Ran, W. Chen, A powerful combination of copper-cysteamine nanoparticles with potassium iodide for bacterial destruction, Mater. Sci. Eng. C 110 (2020) 110659.

[3] K.U. Jansen, C. Knirsch, A.S. Anderson, The role of vaccines in preventing bacterial antimicrobial resistance, Nat. Med. 24 (2018) 10.

[4] C. Rochford, D. Sridhar, N. Woods, Z. Saleh, L. Hartenstein, H. Ahlawat, E. Whiting, M. Dybul, O. Cars, E. Goosby, A. Cassels, G. Velasquez, S. Hoffman, E. Baris, J. Wadsworth, M. GyansaLutterodt, S. Davies, Global governance of antimicrobial resistance, Lancet 391 (2018) 1976–1978.

[5] K.E. Jones, N.G. Patel, M.A. Levy, A. Storeygard, D. Balk, J.L. Gittleman, P. Daszak, Global trends in emerging infectious diseases, Nature 451 (2008) 990–994.

[6] I.B. Seiple, Z. Zhang, P. Jakubec, A. Langlois-Mercier, P.M. Wright, D.T. Hog, K. Yabu, S.R. Allu, T. Fukuzaki, P.N. Carlsen, Y. Kitamura, X. Zhou, M.L. Condakes, F.T. Szczypiński, W.D. Green, A.G. Myers, A platform for the discovery of new macrolide antibiotics, Nature 533 (2016) 338–345.

[7] R. Lopez-Igual, J. Bernal-Bayard, A. Rodriguez-Paton, J.M. Ghigo, D. Mazel, Engineered toxin–intein antimicrobials can selectively target and kill antibiotic-resistant bacteria in mixed populations, Nat. Biotechnol. 37 (2019) 755–760.

[8] R.S. Kalhapure, N. Suleman, C. Mocktar, N. Seedat, T. Govender, Nanoengineered drug delivery systems for enhancing antibiotic therapy, J. Pharmacol. Sci. 104 (2015) 872–905.

[9] L.K. Hidayat, D.I. Hsu, R. Quist, K.A. Shriner, A. Wong-Beringer, High-dose vancomycin therapy for methicillin-resistant Staphylococcus aureus infections: efficacy and toxicity, Arch. Intern. Med. 166 (2006) 2138–2144.

[10] S.P. Chakraborty, S.K. Sahu, S.K. Mahapatra, S. Santra, M. Bal, S. Roy, P. Pramanik, Nanoconjugated vancomycin: new opportunities for the development of anti-VRSA agents, Nanotechnology 21 (2010) 105103.

[11] J. Li, R. Cha, K. Mou, X. Zhao, K. Long, H. Luo, F. Zhou, X. Jiang, Nanocellulose-based antibacterial materials, Adv. Healthcare Mater. 7 (2018) 1800334.

[12] H. Wang, Y. Xu, X. Zhou, Docetaxel-loaded chitosan microspheres as a lung targeted drug delivery system: in vitro and in vivo evaluation, Int. J. Mol. Sci. 15 (2014) 3519–3532.

[13] E.D. Brown, G.D. Wright, Antibacterial drug discovery in the resistance era, Nature 529 (2016) 336–343.

[14] Y. Shi, X.Q. Feng, L.M. Lin, J. Wang, J.Y. Chi, B.Y. Wu, G.L. Zhou, F.Y. Yu, Q. Xu, D. J. Liu, G.L. Quan, C. Lu, X. Pan, J.F. Cai, C.B. Wu, Virus-inspired surface-nanoengineered antimicrobial liposome: a potential system to simultaneously achieve high activity and selectivity, Bioact. Mater. 6 (2021) 3207–3217.

[15] N. Hao, K.W. Jayawardana, X. Chen, M. Yan, One-step synthesis of amine-functionalized hollow mesoporous silica nanoparticles as efficient antibacterial and anticancer materials, ACS Appl. Mater. Interfaces 7 (2015) 1040–1045.

[16] A.G. Kurian, R.K. Singh, K.D. Patel, J.H. Lee, H.W. Kim, Multifunctional GelMA platforms with nanomaterials for advanced tissue therapeutics, Bioact. Mater. 8 (2022) 267–295.

[17] Y. Sun, Y.H. Liu, B.W. Zhang, S.R. Shi, T. Zhang, D. Zhao, T.R. Tian, Q.R. Li, Y. F. Lin, Erythromycin loaded by tetrahedral framework nucleic acids are more antimicrobial sensitive against Escherichia coli (E. coli), Bioact. Mater. 6 (2021) 2281–2290.

[18] J. Zhou, D. Yao, Z. Qian, S. Hou, L. Li, A.T.A. Jenkins, Y. Fan, Bacteria-responsive intelligent wound dressing: simultaneous in situ detection and inhibition of bacterial infection for accelerated wound healing, Biomaterials 161 (2018) 11–23.

[19] Y.Q. Wang, D. Huang, X. Wang, F. Yang, H. Shen, D.C. Wu, Fabrication of zwitterionic and pH-responsive polyacetal dendrimers for anticancer drug delivery, Biomater. Sci. 7 (2019) 3238–3248.

[20] X. Wang, Y.Y. Yang, Y.P. Zhuang, P.Y. Gao, F. Yang, H. Shen, H.X. Guo, D.C. Wu, Fabrication of pH-responsive nanoparticles with an AIE feature for imaging intracellular drug delivery, Biomacromolecules 17 (2016) 2920–2929.

[21] Y. Jaglal, N. Osman, C.A. Omolo, C. Mocktar, N. Devnarain, T. Govender, Formulation of pH-responsive lipid-polymer hybrid nanoparticles for co-delivery and enhancement of the antibacterial activity of vancomycin and 18β-glycyrrhetinic acid, J. Drug Deliv. Sci. Technol. 64 (2021) 102607.

[22] R.S. Kalhapure, M. Jadhav, S. Rambharose, C. Mocktar, S. Singh, J. Renukuntla, T. Govender, pH-responsive chitosan nanoparticles from a novel twin-chain anionic amphiphile for controlled and targeted delivery of vancomycin, Colloids Surf. B Biointerfaces 158 (2017) 650–657.

[23] S.J. Sonawane, R.S. Kalhapure, M. Jadhav, S. Rambharose, C. Mocktar, T. Govender, AB2-type amphiphilic block copolymer containing a pH-cleavable hydrazone linkage for targeted antibiotic delivery, Int. J. Pharm. 575 (2020), 18948.

[24] Z. Azoulay, P. Aibinder, A. Gancz, J. Moran-Gilad, S. Navon-Venezia, H. Rapaport, Assembly of cationic and amphiphilic beta-sheet FKF tripeptide confers antibacterial activity, Acta Biomater. 25 (2021) 231–241.

[25] Y.F. Zuo, X. Wang, Y.Y. Yang, D. Huang, F. Yang, H. Shen, D.C. Wu, Facile preparation of pH-responsive AIE-active POSS dendrimers for detection of trivalent cations and acid gases, Polym. Chem. 7 (2016) 6432–6436.

[26] Y.Z. Bu, L.C. Zhang, J.H. Liu, L.H. Zhang, T.T. Li, H. Shen, X. Wang, F. Yang, P. F. Tang, D.C. Wu, Synthesis and properties of hemostatic and bacteria-responsive in situ hydrogels for emergency treatment in critical situations, ACS Appl. Mater. Interfaces 8 (2016) 12674–12683.

[27] J. Song, B.B. Xu, H. Yao, X.F. Lu, Y. Tan, B.Y. Wang, X. Wang, Z. Yang, Schiff-linked PEGylated doxorubicin prodrug forming pH-responsive nanoparticles with high drug loading and effective anticancer therapy, Front. Oncol. 11 (2021) 656717.

[28] W.G. Liu, M. Wang, W. Cheng, W. Niu, M. Chen, M. Luo, C.X. Xie, T.T. Leng, L. Zhang, B. Lei, Bioactive antiinflammatory antibacterial hemostatic citrate-based dressing with macrophage polarization regulation for accelerating wound healing and hair follicle neogenesis, Bioact. Mater. 6 (2021) 721–728.

[29] B.P. Howden, J.K. Davies, P.D.R. Johnson, T.P. Stinear, M.L. Grayson, Reduced vancomycin susceptibility in staphylococcus aureus, including vancomycin-intermediate and heterogeneous vancomycin-intermediate strains: resistance mechanisms, laboratory detection, and clinical implications, Clin. Microbiol. Rev. 23 (2010) 99–139.

[30] J.T. Mader, M.E. Shirtliff, S.C. Bergquist, J. Calhoun, Antimicrobial treatment of chronic osteomyelitis, Clin. Orthop. Relat. Res. 360 (1999) 47–65.

[31] G.B. Qi, L.L. Li, F.Q. Yu, H. Wang, Vancomycin-modified mesoporous silica nanoparticles for selective recognition and killing of pathogenic gram-positive bacteria over macrophage-like cells, ACS Appl. Mater. Interfaces 5 (2013) 10874–10881.

[32] Y.Q. Shen, E. Jin, B. Zhang, C.J. Murphy, M. Sui, J. Zhao, J.Q. Wang, J.B. Tang, M. H. Fan, E. Van Kirk, W.J. Murdoch, Prodrugs forming high drug loading multifunctional nanocapsules for intracellular cancer drug delivery, J. Am. Chem. Soc. 132 (2010) 4259–4265.

[33] D. Huang, Y.P. Zhuang, H. Shen, F. Yang, X. Wang, D.C. Wu, Acetal-linked pegylated paclitaxel prodrugs forming free-paclitaxel-loaded pH-responsive micelles with high drug loading capacity and improved drug delivery, Mat. Sci. Eng. C 82 (2018) 60–68.

[34] P. Huang, D.L. Wang, Y. Su, W. Huang, Y.F. Zhou, D.X. Cui, X.Y. Zhu, D.Y. Yan, Combination of small molecule prodrug and nanodrug delivery: amphiphilic drug-drug conjugate for cancer therapy, J. Am. Chem. Soc. 136 (2014) 11748–11756.

[35] J.F. Zhang, Z.P. Luo, W.J. Wang, Y.Y. Yang, D.W. Li, Y.Z. Ma, One-pot synthesis of bio-functionally water-soluble POSS derivatives via efficient click chemistry methodology, React. Funct. Polym. 140 (2019) 103–110.
[36] C. Hu, F.J. Zhang, Q.S. Kong, Y.H. Lu, B. Zhang, C. Wu, R.F. Luo, Y.B. Wang, Synergistic chemical and photodynamic antimicrobial therapy for enhanced wound healing mediated by multifunctional light-responsive nanoparticles, Biomacromolecules 20 (2019) 4581–4592.
[37] X. Wang, P.Y. Gao, Y.Y. Yang, H.X. Guo, D.C. Wu, Dynamic and programmable morphology and size evolution via a living hierarchical self-assembly strategy, Nat. Commun. 9 (2018) 2772.
[38] Z.W. Liu, X.Y. Zhao, B.R. Yu, N.N. Zhao, C. Zhang, F.J. Xu, Rough Carbon−iron oxide nanohybrids for near-infrared-II light-responsive synergistic antibacterial therapy, ACS Nano 15 (2021) 7482–7490.